



Hot deformation behaviour of 7075 alloy

M. Rajamuthamilselvan*, S. Ramanathan

Department of Manufacturing Engineering, Annamalai University, Annamalai Nagar, Mayiladuthurai, Tamil Nadu, 608002, India

ARTICLE INFO

Article history:

Received 6 March 2010

Received in revised form

21 September 2010

Accepted 26 September 2010

Available online 7 October 2010

Keywords:

Processing map

Hot deformation

Dynamic recrystallization

Flow curve

ABSTRACT

The hot deformation behaviour of Stir cast 7075 alloy was studied using processing map technique. The map has been interpreted in terms of the microstructural processes occurring in situ with deformation, based on the values of a dimensionless parameter η which is an efficiency index of energy dissipation through microstructural processes. An instability criterion has also been applied to demarcate the flow instability regions in the processing map using another parameter (ξ). Both the parameters (η and ξ) were computed from the experimental data generated by compression tests conducted at various temperatures and strain rate combinations over the hot working range (300–500 °C and 0.001–1.0 s⁻¹) of the present material. The processing map exhibits one distinct η domains without any unstable flow conditions under the investigated temperature and strain rate conditions. The dynamic recrystallization zone and instable zones, i.e. adiabatic shear band formation, interface crack, and wedge cracking, were identified in the processing map. Microstructural examination was performed for validation. The processing maps can be used to select optimum strain rates and temperatures for effective hot deformation of 7075 alloy.

© 2010 Elsevier B.V. All rights reserved.

1. Introduction

High strength to weight ratio aluminium (Al) and its alloys find their potential application in various automobile and aerospace components [1,2]. The mechanical properties are closely related to the microstructure of these alloys, which are greatly influenced by thermo mechanical processing. So it is necessary to research the effects of thermo mechanical parameters, such as deformation temperature and strain rate, on the microstructure of high-strength aluminium alloy. During high-temperature deformation of aluminium alloys with high-stacking fault energy, boundary misorientation angle is an important characterization parameter of microstructures [3].

Bulk metalworking processes are carried out at elevated temperatures where the occurrence of simultaneous softening process would enable the imposition of large strains in a single step or multiple steps. Hot working also causes a significant change in the microstructure of the material and this contributes to one part of workability generally referred to intrinsic workability [4], which is sensitive to initial conditions and the process parameters. The workability may be improved to facilitate further processing. An understanding of constitutive behaviour of the material is essential for the optimization of the intrinsic workability and control of microstructural evolution during hot working. This is done using trial and error techniques which are both expensive and time con-

suming and may not lead to successful solution or optimization. Hence, the trial and error techniques are replaced with material modeling which are developed on science based principles [4].

Dynamic materials modeling, first developed by Prasad and Sasidhara [5], is based on fundamental properties of continuum mechanics of large plastic flow, physical system modeling, and irreversible thermodynamics. In this model, the work piece during hot deformation is considered to be a dissipater of power. The dissipated power is converted into thermal and microstructural forms.

The processing map technique has been widely used to understand the hot workability of many materials in terms of microstructural processes operating over a range of temperatures and strain rates [6,7]. The processing map technique is based on the dynamic materials model (DMM), which considers the complementary relationship between the rate of visco-plastic heat generation induced by deformation and the rate of energy dissipation associated with microstructural changes occurring during deformation. A systematic understanding of its effects on hot deformation behaviour will enable processing with microstructure and property control. The processing window for a given material is conventionally established on the basis of workability parameters such as ductility, efficiency of power dissipation, flow localization parameter, instability criteria, apparent activation energy, and/or existence of favorable microstructural mechanisms like dynamic recrystallization (DRX), dynamic recovery (DRY), or super plasticity. The deformation process is considered to be stable if it does not cause inhomogeneous flow or instabilities (e.g. flow localization, dynamic strain aging, adiabatic shear banding, and macro/micro cracking).

* Corresponding author. Tel.: +91 9486472483; fax: +91 4144239734.
E-mail address: rajanarmi@yahoo.co.in (M. Rajamuthamilselvan).

The present work is initiated to study the hot working characteristics of 7075Al alloy at different temperatures and strain rates. The processing map was generated.

2. Experimental studies

2.1. Stir casting of Al alloy

Stir casting technique was used to fabricate 7075Al alloy. The material was 7075 aluminium alloy (composition in wt% Cu 1.66, Mg 2.10, Si 0.14, Mn 0.21, Fe 0.40, Cr 0.18, Zn 5.67, Ti 0.01 and rest Al). The aluminium alloy was melted by using an electric furnace and poured in permanent mould. The cast billets were soaked in the temperature of 400 °C for 30 min and hot extruded. The cylindrical specimens of dimensions, 10 mm in diameter and 10 mm in height were machined from the extruded rods.

The hot compression tests [8] were performed on a 10T servo controlled universal testing machine for different strains (0.1–0.5), strain rates (0.001–1.0 s⁻¹) and temperatures (300–500 °C). Temperature of the specimen was monitored with the aid of a chromel/alumel thermocouple embedded in a 0.5 mm hole drilled half the height of the specimen as stated by Prasad and Rao [9]. The thermocouple was also used for measuring the adiabatic temperature rise in the specimen during deformation. The specimens were effectively lubricated with graphite and deformed to a true strain of 0.5. After compression testing, the specimens were immediately quenched in water and the cross section was examined for microstructure. Specimens were deformed to half of the original height. Deformed specimens were sectioned parallel to the compression axis and the cut surface was prepared for metallographic examination. Specimens were etched with Keller's solution. The microstructure of the specimens was obtained through Versamet 2.0 optical microscope with Clemex vision Image Analyser and mechanism of deformation was studied. Using the flow stress data, power dissipation efficiency and flow instability were evaluated for different strain rates, temperatures at a constant strain of 0.5. The processing maps were developed for 0.5 strains for 7075Al alloy.

2.2. Determination of deformation parameters

The deformation behaviour of any metallic material is governed by the internal constitution of the material and the rate of strain hardening. The strength of materials increases with increase in the plastic strain rate. The rate sensitive flow behaviour is given by [10,11]

$$\sigma = K\dot{\epsilon}^m \quad (1)$$

where K is a parameter that depends upon structure of the material and temperature and, m is the strain rate sensitivity parameter. The value of m is determined by a variant of Eq. (1) given at a constant strain and temperature [12]

$$m = \frac{\partial \log \sigma}{\partial \log \dot{\epsilon}} \Big|_{\epsilon, T} \quad (2)$$

The deformation behaviour of composites is influenced by the complexity of the dynamic microstructural processes. This can be understood by using activation energy (Q) for microstructural mechanisms that relates the steady state flow stress (σ) with applied strain rate ($\dot{\epsilon}$) and temperature (T) by an Arrhenius-type rate equation given as [13,14]

$$\dot{\epsilon} = A\sigma^n e^{-Q/RT} \quad (3)$$

where A is a constant, n the stress exponent, that is also equal to $1/m$ [14], R the gas constant and Q the activation energy. At a given strain rate, the slope of the $\log \sigma$ and $\log(1/T)$ gives the activation energy.

The deformation process is accompanied by two power dissipation routes (1) the power required to bring in microstructural changes in the work piece and (2) the dissipation in heat generation during deformation. For an ideal plastic flow, the flow stress is proportional to the strain rate at any strain and temperature. The efficiency is defined as the ratio of the heat dissipated in the microstructural changes and the maximum dissipation possible the efficiency of deformation is thus given by [10,12]

$$\eta = \frac{2m}{m+1} \quad (4)$$

where ' m ' is the strain rate sensitivity of the material, which is a function of deformation temperature and strain rate. The iso-efficiency contour plot on the temperature–strain rate field constitutes the processing map. Several domains can be identified in the map based on the η contours (i.e. power dissipation characteristics), each of them representing a dominant deformation mechanism. The peak efficiency condition of the domain corresponds to the optimum deformation condition. In addition to the η contours, the instability criterion given by the following equation (5) [15]:

$$\xi(\dot{\epsilon}) = \frac{\delta \ln(m/m+1)}{\delta \ln \dot{\epsilon}} + m < 0 \quad (5)$$

is applied to delineate the temperature strain rate regimes of flow instability on the processing map.

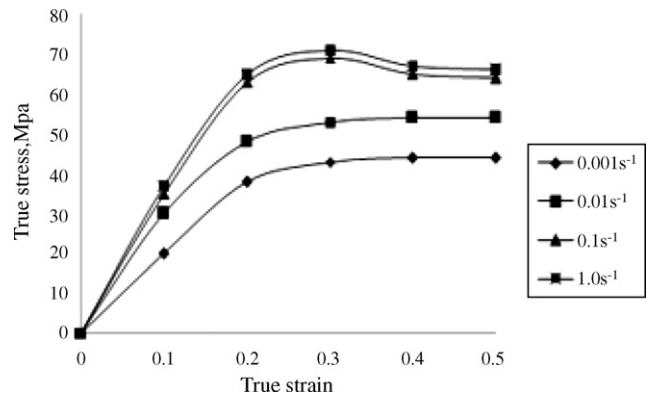


Fig. 1. The flow curves for different strain rates at constant temperature of 350 °C.

3. Results and discussion

The hot compression tests were performed on 7075 aluminium alloy with temperature range of 300–500 °C and strain rate range of 0.001–1.0 s⁻¹ in different strains (0.1–0.5). Flow stress data has been obtained from the load–stroke data.

The rate at which strain is applied to a specimen can have an important influence on the flow stress. The flow stress decreased with an increase in temperature and a decrease in strain rate. For different strain rates, the configuration of each flow curves is different. The flow stress is affected by many factors, such as alloying composition, microstructure, deformation mode, temperature and deformation by power expression of the form in Eq. (1).

The input to generate a processing map is the experimental data of flow stress as a function of temperature, strain rate and strain. As the map generated will be only as good as the input data, it is important to use accurate, reliable and yet simple experimental technique for generating them. In general, the material starts “flowing” or deforming plastically when the applied stress (in uniaxial tension without necking or in uniaxial compression without bulging) reaches the value of the flow stress. While hot tensile, hot torsion or hot compression testing techniques may be used for this purpose, hot compression test has decisive advantages over others. In a compression test on a cylindrical specimen, it is easy to obtain a constant true strain rate using an experimental decay of the actuator speed. It is convenient to measure the adiabatic temperature rise directly on the specimen and conduct the test under isothermal conditions.

3.1. Interpretation from flow stress–flow strain curves

Flow stresses to divide the characteristics of metal flows occurred for dynamic recovery and recrystallization, counting initial austenite grain size obtained from numerous experiments. When the material is able to dissipate the provided power through the load transfer or through metallurgical transformations it does not reach high levels of damage [16].

The flow curves obtained for 7075Al alloy deformed in compression at 350 °C at different strain rates ranging from 0.001 to 1.0 s⁻¹ are presented in Fig. 1. The flow stress is significantly low at lower strain rates whereas the work hardening rate is relatively high. Hence the flow stress is found to increase with increase in strain. At lower strain rates, the deformation is isothermal but at high strain rates it is adiabatic. At lower strain rates, oscillations are observed in the flow stress. The oscillations are not readily apparent since the noise in the data sometimes proved to be of larger amplitude than the oscillations themselves [17]. The flow stress–flow strain curves exhibit flow softening at higher strain rates. The rise in temperature leads to decrease in work hardening rate.

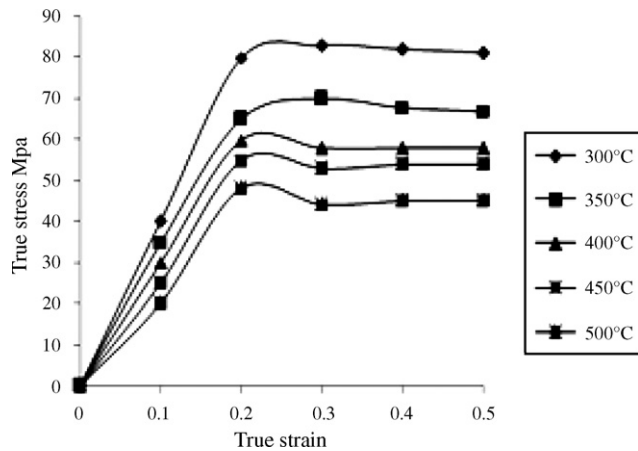


Fig. 2. The flow curves for different temperatures at constant strain rate of 0.1 s^{-1} .

The flow curves for different temperatures and constant strain rates at 0.1 s^{-1} are shown in Fig. 2. It can be seen that the true stress–true strain curves exhibit a peak stress at certain strain, followed by dynamic flow softening until the end of compression. The peak stress and flow stress increase with increasing strain rate and with decreasing deformation temperature. The strain corresponding to the peak stress increases with increase in strain rate and/or with decrease in deformation temperature due to the high hardening rate at initial deformation stages. The flow softening is probably subjected to the dynamic recovery and recrystallization, as well as dynamic coarsening of precipitates during hot deformation of aluminium alloys [18,19].

3.2. Interpretation from processing map

Material flow behaviour for defining deformation processing maps that delineate “safe” and “non-safe” hot working conditions. These maps show in the processing space, i.e. on the axes of temperature and strain rate, the processing conditions for stable and unstable deformation. The large stable region compares well with the ‘safe’ processing region for commercial purity aluminium in Raj’s atomistic mechanism map [20]. The processing map obtained at a strain of 0.5 (steady state plastic flow) is shown in Fig. 3. The numbers against each contour represent the efficiency of power dissipation as percent. The thick line represents the boundary for the regime of flow instability as per the criterion given in Eq. (5). The map exhibits a single domain in the temperature range $350\text{--}395^\circ\text{C}$

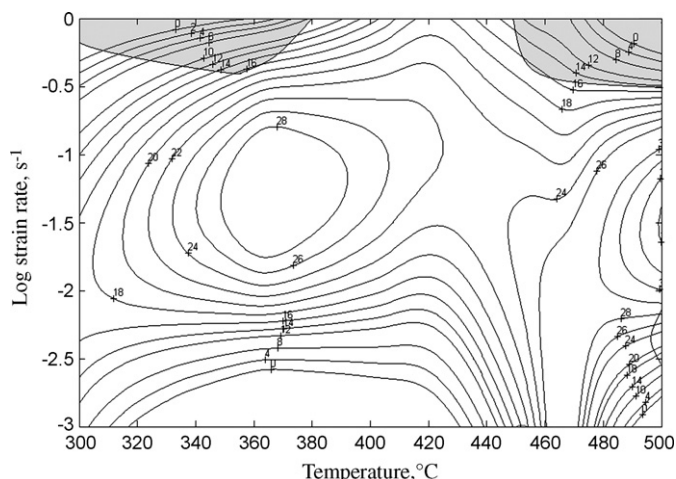


Fig. 3. Processing map for 7075 alloy at 0.5 strain.

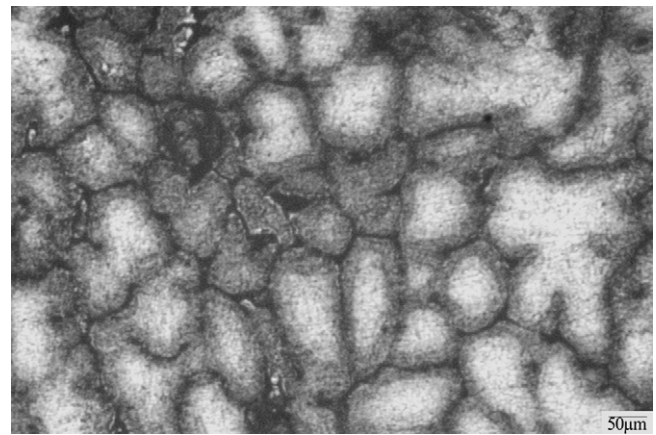


Fig. 4. Dynamic recrystallization at 350°C at a strain rate of 0.1 s^{-1} .

and strain rate range $0.013\text{--}0.12 \text{ s}^{-1}$ with a peak efficiency of about 28% occurring at 350°C and 0.1 s^{-1} . The stable efficiency value as a function of strain indicates that the power dissipation is through equilibrium microstructural processes occurring during deformation, namely the dynamic restoration processes such as DRX, DRV and extended DRV.

3.3. Microstructural examination

The deformation process is said to be “stable” if the deforming material does not exhibit any inhomogeneous deformation and flow instability. Since the deformation is uniform in the stable regions the behaviour of the materials is deterministic and can be modeled accurately. These microstructural models can be used for microstructural control during the manufacture of the components.

DRX, DRV processes involve in situ dislocation generation and annihilation with deformation, which attain equilibrium state with strain. As these processes are less effective in dissipating power compared to fracture processes, the efficiency associated with the plateau domain is comparatively less. DRX takes place at lower temperatures or/and higher strain rates. After reaching the critical strain the nucleation and growth of the small and equiaxed grains take place. In the initial stage of hot formation process, the sub grains grow by boundary migration and coalescence. With increasing strain, new recrystallized grains deform by high-angle grain boundary migration. Under this condition, it takes a longer time (and the greater strain) to accumulate the critical dislocation density needed to trigger recrystallization. Recrystallization “waves” pass through the material. As a low dislocation density is the characteristic of each individual grain, the overall stress level corresponds to the lower line approximately [21]. The DRX zone obtained during testing at a temperature of 350°C and strain rate of 0.1 s^{-1} is shown in Fig. 4. These observations reveal that the range from 0.013 to 0.12 s^{-1} is the DRX domain. It is safe for bulk metal processing. The optimum range for bulk metal processing in the safe domain as obtained from the processing map is $360\text{--}460^\circ\text{C}$ at the strain rate of $0.01\text{--}0.1 \text{ s}^{-1}$. Prasad et al. [22] explained that the materials with stable fine-grained structure when deformed at slow speeds and high temperature exhibit abnormal elongations and the process is called super plasticity. The grain elongation is identified at the temperature 350°C and at a strain rate of 0.1 s^{-1} , which is shown in Fig. 5.

The phenomena which cause inhomogeneous deformation during forming can be termed as “flow instabilities” and the regimes of temperature and strain rate where deformation is not homogeneous can be termed as “unstable” or “instability” regions.

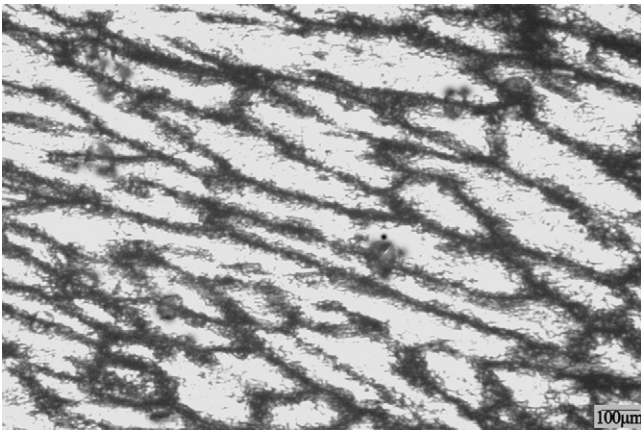


Fig. 5. Grain elongation at 350 °C and a strain rate of 0.1 s⁻¹.

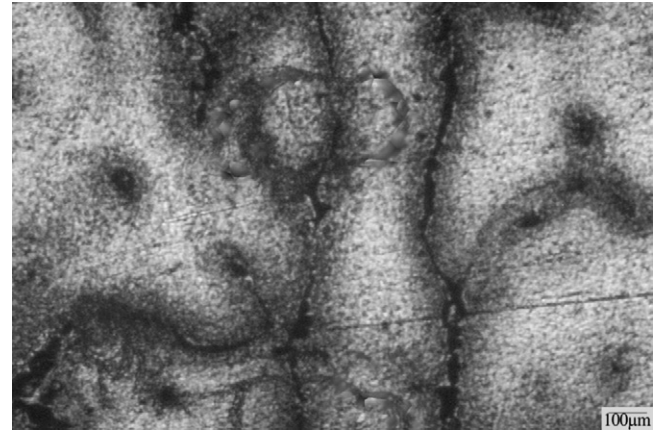


Fig. 7. Interface crack at 500 °C and at a strain rate of 1.0 s⁻¹.

At higher strain rates, adiabatic deformation heat generated during hot working is not conducted due to insufficient time and low thermal conductivity, inducing highly localized flow along the maximum shear stress plane [23]. That process is called as adiabatic shear band formation. It is being observed at an angle of about 45° to the compressive axis. The shear band formation alignment along the shear directions are observed in Fig. 6 at the temperature of 300 °C and strain rate of 1.0 s⁻¹.

Super plastic deformation may cause interface cracking. This may lead to the creation of microstructural damage due to cavity formation ultimately contributing to ductile fracture. The energy dissipation is through the formation of new surfaces and in general this is highly efficient, though not desirable, process. This influence of temperature and strain rate is greater in this process, and this domain is undesirable for processing and hence should be avoided [24]. This type of observations is seen in Fig. 7 (interface crack) (temperature of 500 °C and strain rate of 1.0 s⁻¹).

Materials with a stable fine grain structure when deformed at elevated temperatures and slow speeds, exhibit abnormal elongation. The process is termed as super plastic deformation which basically consists of grain boundary sliding with a simultaneous occurrence of diffusion, accommodated flow at a rate that can repair the wedge cracks forming at grain boundary triple junctions. Prasad et al [25] reported that the wedge cracking occurs at higher temperature and lower strain rate. The consequence of the grain boundary sliding process depends upon the accommodation mechanism at the grain boundary triple junctions, where considerable stress concentration is caused by the sliding of the neighboring grains. If the rate of stress concentration is beyond the rate of matching and the

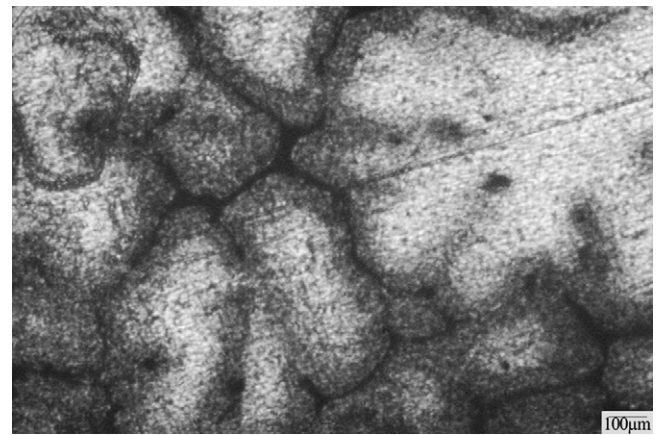


Fig. 8. Wedge cracking at 450 °C and at a strain rate of 0.001 s⁻¹.

rate of grain boundary sliding, wedge cracking will occur. Fig. 8 shows the microstructure of wedge cracking at a temperature of 450 °C and strain rate of 0.001 s⁻¹.

4. Conclusions

The hot deformation behaviour of 7075 aluminium alloy has been studied by employing hot compression tests in the temperature and strain ranges of 300–500 °C and 0.001–1.0 s⁻¹ respectively. The processing map is used to select optimum domains for effective hot deformation of 7075 alloy.

Dynamic recrystallization occurs in the temperature range of 340–390 °C and strain rate range of 0.013–0.12 s⁻¹. The optimum processing parameters for hot working of 7075 aluminium alloy is 350 °C and 0.1 s⁻¹ having efficiency of 28%, is identified.

At higher strain rate, the material exhibits flow instability such as adiabatic shear band and matrix cracking in the temperature range of 300–380 °C and 440–500 °C respectively. Also wedge cracking is obtained in the higher temperature range of 490–500 °C and lower strain rate. These temperatures and strain rates should be avoided in processing the material.

Acknowledgements

The authors are grateful to the Department of Manufacturing Engineering, Annamalai University, Tamil Nadu, India for the support rendered for the fabrication and testing of composites.

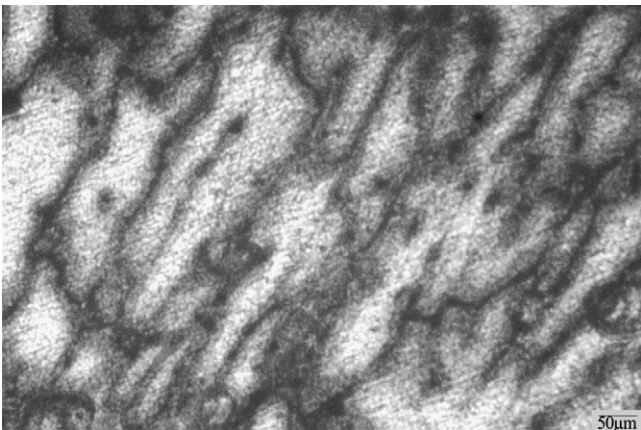


Fig. 6. Adiabatic shear band formation at 300 °C and at a strain rate of 1.0 s⁻¹.

References

- [1] J.C. Williams, E.A. Starke, *Acta Mater.* 51 (19) (2003) 5775–5799.
- [2] J. Wloka, T. Hack, S. Virtanen, *Corros. Sci.* 49 (3) (2007) 1437–1449.
- [3] B. Han, Z. Xu, *Mater. Sci. Eng. A* 447 (2007) 119–124.
- [4] S. Ramanathan, R. Karthikeyan, G. Ganaseen, *Mater. Sci. Eng. A* 441 (2006) 321–325.
- [5] Y.V.R.K. Prasad, S. Sasidhara, *Hot Working Guide*, ASM International, 1997.
- [6] N. Srinivasan, Y.V.R.K. Prasad, P. Ramarao, *Mater. Sci. Eng. A* 476 (2008) 146–156.
- [7] G. Zbigniew, *J. Mater. Process. Technol.* 159 (2005) 377–382.
- [8] Y.C. Lin, M.-S. Chen, J. Zhong, *Mech. Res. Commun.* 35 (3) (2008) 142–150.
- [9] Y.V.R.K. Prasad, K.P. Rao, *Mater. Sci. Eng. A* 391 (2005) 141–150.
- [10] S.V.S. Narayana Murty, B. Nageswara Rao, B.P. Kashyap, *Compos. Sci. Technol.* 63 (2003) 119–135.
- [11] Y.H. Frank Su, Y.C. Chen, C.Y.A. Tsao, *Mater. Sci. Eng. A* 364 (2004) 296–304.
- [12] P. Cavaliere, E. Evangelista, *Compos. Sci. Technol.* 66 (2006) 357–362.
- [13] G. Ganesan, K. Raghukandan, R. Kartikeyan, B.C. Pai, *Mater. Sci. Eng. A* 369 (2004) 230–235.
- [14] S. Das, V.S.R. Murthy, G.S. Murthy, *Bull. Mater. Sci.* 24 (2001) 215–218.
- [15] S.H. Mousavi Anijdan, H.R. Madaah-Hosseini, A. Bahrami, *Mater. Des.* 28 (2007) 609–615.
- [16] S. Spigarelli, E. Cerri, P. Cavaliere, E. Evangelista, *Mater. Sci. Eng. A* 327 (2002) 144–154.
- [17] K.P. Rao, K. Ramkumar, Oruganti, J. *Mater. Process. Technol.* 138 (2003) 97–101.
- [18] H.E. Hu, L. Zhen, L. Yang, W.Z. Shao, B.Y. Zhang, *Mater. Sci. Eng. A* 488 (2008) 64–71.
- [19] H. Zhang, L. Li, D. Yuan, D. Peng, *Mater. Charact.* 58 (2007) 168–173.
- [20] R. Raj, *Metall. Trans.* 12A (1981) 1089–1094.
- [21] J. Liu, Z. Cui, C. Li, *Comp. Mater. Sci.* 41 (2008) 375–382.
- [22] Y.V.R.K. Prasad, T. Seshacharyalu, S.C. Medeiros, W.G. Frazier, *Mater. Sci. Technol.* 16 (2000) 511–520.
- [23] A.B. Li, L.J. Huang, Q.Y. Meng, L. Geng, X.P. Cui, *Mater. Des.* 30 (2009) 1625–1631.
- [24] O. Sivakesavam, Y.V.R.K. Prasad, *Mater. Sci. Eng. A* 323 (2002) 270–277.
- [25] Y.V.R.K. Prasad, T. Seshacharyalu, S.C. Medeiros, W.G. Frazier, *Mater. Sci. Eng. A* 279 (2000) 289–299.